Archives of Control Sciences
Volume 17(LIII), 2007
No. 3, *pages 271–282*

A novel method for vibration surveillance during high speed ball end milling of flexible details

KRZYSZTOF J. KALIŃSKI

The paper is devoted to vibration surveillance of unsteady systems, which are idealized by the finite element method. Ball end milling of flexible details is observed very frequently in case of modern machining centres. Tool-workpiece relative vibration may lead to a loss of stability and cause a generation of self-excited *chatter* vibration. The paper proposes the method of minimizing vibration level, based on matching the spindle speed to the optimal phase shift. As result of a milling process modeling, we get a hybrid system in which are separated:

- Modal subsystem. It is a stationary model of one-side-supported flexible detail.
- Structural subsystem, i.e. non-stationary discrete model of ball end mill and cutting process.
- Connective subsystem as conventional contact point between tool and workpiece.

The method has been developed with success. Modal model of the workpiece allowed us to determine an optimal spindle speed. Modal assurance criterion (*MAC*) has been assessed and confirmed good agreement between experimental and theoretical modal model. Results of computer simulation, as well as - of experimental investigation on the Mikron VCP 600 milling machine mean to be in support. Hence amplitude values for chosen optimal spindle speed became relatively smaller than for the other ones.

Key words: high speed cutting, dynamics, vibration control, hybrid systems

1. Introduction

In case of modern machining centres, ball end milling of flexible details is observed very frequently. It is obvious that tool-workpiece relative vibration plays principal role during cutting process. Due to existence of certain conditions, it may lead to a loss of stability and cause a generation of self-excited chatter vibration [1]. Some methods of the chatter reduction depended on the programmed spindle speed control [2, 3], the spindle speed optimal control [2, 4] and the spindle speed optimal-linear control [5]. Results

---

K. Kaliński is with Faculty of Mechanical Engineering, Gdańsk University of Technology, Gdańsk, Poland. E-mail: kkalinsk@o2.pl

Experimental verification has been performed thanks to The Plant of Design of Machines and Production Equipment ‘LONZA’ in Gdansk, Poland, as well as to Ecole Nationale d’Ingenieurs de Metz, France.

The research was supported by The Polish Ministry of Education and Science, Grant No. 5 T07C 037 25 and subjective subvention (decision no. 155/E-359/SPB/Cooperation with FP UE/DIE 485/2004).

Received 20.11.2007.

of further research have disclosed that milling flexible billets at changing spindle speed appears unsuccessful however, with respect to vibration surveillance. Thus, the paper proposes the other method of minimising vibration level, which is based on matching the spindle speed to the optimal phase shift [6].

2. Cutting process dynamics

Dynamic analysis of a slender ball end milling process has been performed, based upon following assumptions [2].

- The spindle together with the tool fixed in the holder, and the table with the workpiece, are separated from the machine tool's structure.
- Here is considered flexibility of the tool and flexibility of the workpiece.
- Position between symmetry axis of the tool and feed speed v_f, refers to the pulling milling. The latter prevents from cutting at contribution of the ball end mill top.
- Coupling elements (CEs) are applied for modelling the cutting process.
- An effect of first pass of the edge along cutting layer causes proportional feedback, but the effect of multiple passes causes delayed feedback additionally.

As result of a milling process modelling, we get a hybrid system, in which are separated (Fig. 1 and 2):

- modal subsystem. It is a stationary model of one-side-supported flexible plate, which displaces itself with desired feed speed v_f;
- structural subsystem, that is to say non-stationary discrete model of ball end mill (speed of revolution n) and cutting process;
- abstractive connective subsystem as conventional contact point S between tool and workpiece.

For instantaneous contact point between chosen tool edge and the workpiece (idealised by CE no. l), proportional model of the cutting dynamics is included [1, 2]. Thus, we can describe following components of instantaneous cutting force:

$$F_{yl1}(t) = \begin{cases} k_{dl} a_p [h_{Dl}(t) - \Delta h_i(t) + \Delta h_l(t-\tau_l)], \\ h_{Dl}(t) - \Delta h_l(t) + \Delta h_l(t-\tau_l) > 0, \\ 0, \\ h_{Dl}(t) - \Delta h_l(t) + \Delta h_l(t-\tau_l) \leqslant 0, \end{cases} \tag{1}$$

$$F_{yl2}(t) = \begin{cases} \mu_l k_{dl} a_p [h_{Dl}(t) - \Delta h_i(t) + \Delta h_l(t - \tau_l)], \\ h_{Dl}(t) - \Delta h_l(t) + \Delta h_l(t - \tau_l) > 0, \\ 0, \\ h_{Dl}(t) - \Delta h_l(t) + \Delta h_l(t - \tau_l) \leqslant 0, \end{cases} \tag{2}$$

$$F_{yl3}(t) = 0 \tag{3}$$

where: k_{dl} – average dynamic specific cutting pressure,
$h_{Dl}(t)$ – desired cutting layer thickness; $h_{Dl}(t) \approx f_z \cos\varphi_l(t)$,
$\Delta h_l(\cdot)$ – dynamic change in cutting layer thickness,
μ_l – cutting force ratio (a quotient of forces F_{yl2} and F_{yl1}),
τ_l – time-delay between the same position of CE no. l and CE no. $l-1$,
f_z – feed per tooth.

As result of transformation of generalized displacements to co-ordinate system x_{1e}, x_{2e}, x_{3e}, matrix equation of the discrete system's dynamics shall get a form [2]:

$$\boldsymbol{M}\ddot{\boldsymbol{q}} + \boldsymbol{L}\dot{\boldsymbol{q}} + \boldsymbol{K}^*\boldsymbol{q} = \boldsymbol{f}^* \tag{4}$$

where:
$\boldsymbol{K}^*(t) = \boldsymbol{K} + \sum_{l=1}^{i_l} \boldsymbol{T}_l^T(t)\boldsymbol{D}_{Pl}\boldsymbol{T}_l(t)$,
$\boldsymbol{f}^* = \sum_{l=1}^{i_l} \boldsymbol{T}_l^T(t)\boldsymbol{F}_l^0(t) + \sum_{l=1}^{i_l} \boldsymbol{T}_l^T(t)\boldsymbol{D}_{Ol}\boldsymbol{\Delta w}_l(t-\tau_l)$,

$\boldsymbol{q}$ – vector of generalized displacements of the system,
$\boldsymbol{M}$, $\boldsymbol{L}$, $\boldsymbol{K}$ – matrices of inertia, damping and stiffness of decoupled system (i.e. the slender ball end mill alone),
$\boldsymbol{F}_l^0(t)$ – vector of desired forces of CE no. l,
$\boldsymbol{D}_{Pl}$, $\boldsymbol{D}_{Ol}$ – matrices of proportional and delayed feedback of CE no. l,
$\boldsymbol{\Delta w}_l(t-\tau_l)$ – vector of deflections of CE no. l for time-instant $t-\tau_l$.

The matrix of transformation $T_l(t)$ is time-dependent, because several edges of the cutter change their positions ourselves.

3. Dynamics of flexible details as of a hybrid system

Further consideration concerns the system's decomposition into several ones.

1. Modal subsystem, whose behavior is described in domain of generalized co-ordinates $\boldsymbol{q}_m$. Matrices of inertia, damping and stiffness are $\boldsymbol{M}_{mm}$, $\boldsymbol{L}_{mm}$, $\boldsymbol{K}_{mm}$, but vector of generalized forces is $\boldsymbol{f}_m$. Properties of that subsystem are defined by:

$$\boldsymbol{\Omega}_m = \mathrm{diag}[\omega_{01}\ \omega_{02}\ \ldots\ \omega_{0mod}]$$

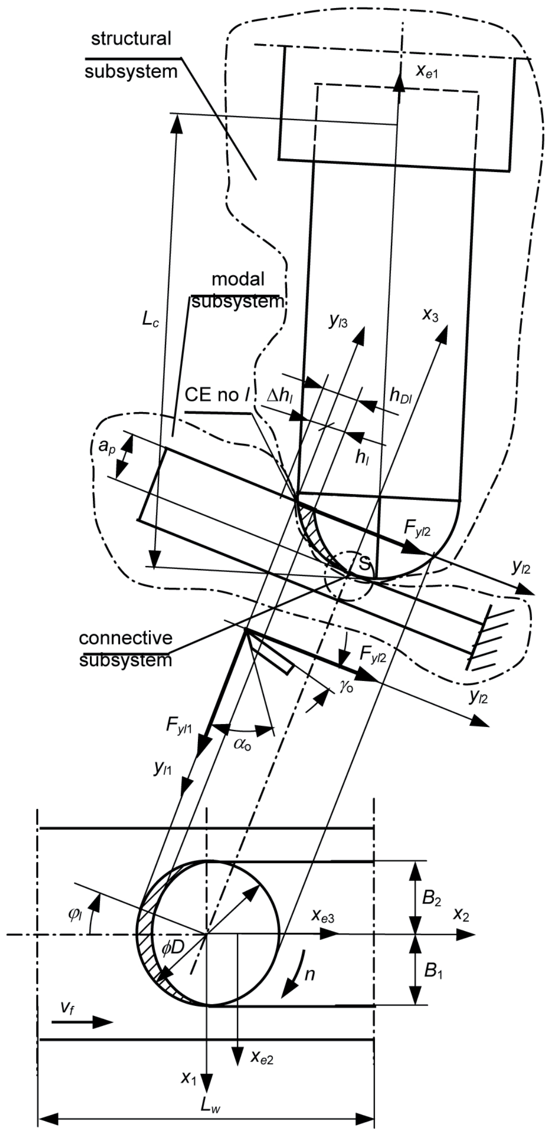

Figure 1. A scheme of a slender ball end milling of one-side-supported flexible plate.

– matrix of undamped angular natural frequencies ω_{0k}, $k = 1, \ldots, mod$,

$$\mathbf{\Psi}_m = [\Psi_1 \; \Psi_2 \; \ldots \; \Psi_{0mod}]$$

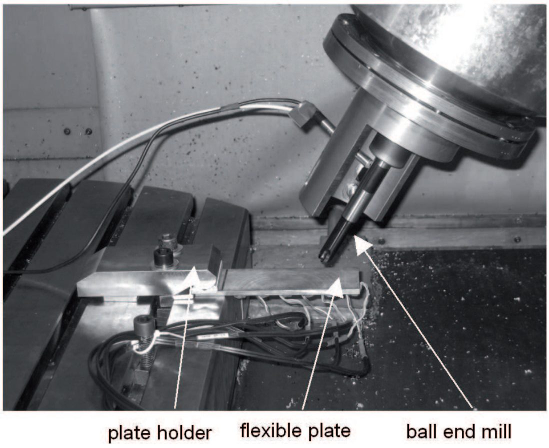

Figure 2. View of a slender ball end milling of one-side-supported flexible plate.

– matrix of normal modes Ψ_k corresponding to undamped angular frequencies of the system ω_{0k}, $k = 1, \dots, mod$,

$$\boldsymbol{Z}_m = \mathrm{diag}[\zeta_1\ \zeta_2\ \dots\ \zeta_{mod}]$$

– matrix of dimensionless damping coefficients corresponding to modes $k = 1, \dots, mod$, mod is a number of modes being considered.

Let us suppose that following conditions are fulfilled.

$$\boldsymbol{q}_m = \boldsymbol{\Psi a}_m, \tag{5}$$

$$\boldsymbol{\Psi}_m^T \boldsymbol{M}_{mm} \boldsymbol{\Psi}_m = \boldsymbol{I}_m, \tag{6}$$

$$\boldsymbol{\Psi}_m^T \boldsymbol{L}_{mm} \boldsymbol{\Psi}_m = 2\boldsymbol{Z}_m \boldsymbol{\Omega}_m, \tag{7}$$

$$\boldsymbol{\Psi}_m^T \boldsymbol{K}_{mm} \boldsymbol{\Psi}_m = \boldsymbol{\Omega}_m^2. \tag{8}$$

2. Structural subsystem, whose behavior is described in domain of generalized co-ordinates $\boldsymbol{q}_s$.

3. Connective subsystem, whose domain is vector of generalized co-ordinates $\boldsymbol{q}_c$.

It is assumed that rheonomic-holonomic constraints appear between generalized co-ordinates of modal subsystem $\boldsymbol{q}_m$ and of connective subsystem $\boldsymbol{q}_c$. Thus we can write:

$$\boldsymbol{W}_c \boldsymbol{q}_c = \boldsymbol{W}_m \boldsymbol{q}_m \quad \text{or} \quad \boldsymbol{q}_c = \boldsymbol{W q}_m, \tag{9}$$

where: $\boldsymbol{W} = (\boldsymbol{W}_c^T \boldsymbol{W}_c)^{-1} \boldsymbol{W}_c^T \boldsymbol{W}_m = \boldsymbol{W}(t)$.

Note, that the free-off-constraints system (even non-stationary) becomes stationary. Besides, one ought to focus a special attention on size of matrix $\boldsymbol{W}_c$, in which number of rows should not be smaller than number of columns. Otherwise, the matrix product in brackets appears singular. Hence the latter is impossible to be inverted.

If we consider constraint reactions' equation, constraints' equations and their time derivatives, we shall get description of dynamics of non-stationary system in hybrid co-ordinates ξ, that is to say:

$$\boldsymbol{M}_{\xi}\ddot{\boldsymbol{\xi}} + \boldsymbol{L}_{\xi}\dot{\boldsymbol{\xi}} + \boldsymbol{K}_{\xi}\boldsymbol{\xi} = \boldsymbol{f}_{\xi}, \tag{10}$$

where:

$$\boldsymbol{M}_{\xi} = \begin{bmatrix} \boldsymbol{I}_m + \boldsymbol{\Psi}_m^T\boldsymbol{W}^T\boldsymbol{M}_{cc}\boldsymbol{W}\boldsymbol{\Psi}_m & \boldsymbol{\Psi}_m^T\boldsymbol{W}^T\boldsymbol{M}_{cs} \\ \boldsymbol{M}_{cs}\boldsymbol{W}\boldsymbol{\Psi}_m & \boldsymbol{M}_{ss} \end{bmatrix},$$

$$\boldsymbol{L}_{\xi} = \begin{bmatrix} 2\boldsymbol{Z}_m\boldsymbol{\Omega}_m + 2\boldsymbol{\Psi}_m^T\boldsymbol{W}^T\boldsymbol{M}_{cc}\dot{\boldsymbol{W}}\boldsymbol{\Psi}_m + \boldsymbol{\Psi}_m^T\boldsymbol{W}^T\boldsymbol{L}_{cc}\boldsymbol{W}\boldsymbol{\Psi}_m & \boldsymbol{\Psi}_m^T\boldsymbol{W}^T\boldsymbol{L}_{cs} \\ 2\boldsymbol{M}_{sc}\dot{\boldsymbol{W}}\boldsymbol{\Psi}_m + \boldsymbol{L}_{sc}\boldsymbol{W}\boldsymbol{\Psi}_m & \boldsymbol{L}_{ss} \end{bmatrix},$$

$$\boldsymbol{K} = \begin{bmatrix} \boldsymbol{\Omega}^2 + \boldsymbol{\Psi}_m^T\boldsymbol{W}^T\boldsymbol{M}_{cc}\ddot{\boldsymbol{W}}\boldsymbol{\Psi}_m + \boldsymbol{\Psi}_m^T\boldsymbol{W}^T\boldsymbol{L}_{cc}\dot{\boldsymbol{W}}\boldsymbol{\Psi}_m + \boldsymbol{\Psi}_m^T\boldsymbol{W}^T\boldsymbol{K}_{cc}\boldsymbol{W}\boldsymbol{\Psi}_m & \boldsymbol{\Psi}_m^T\boldsymbol{W}^T\boldsymbol{K}_{cs} \\ \boldsymbol{M}_{sc}\ddot{\boldsymbol{W}}\boldsymbol{\Psi}_m + \boldsymbol{L}_{sc}\dot{\boldsymbol{W}}\boldsymbol{\Psi}_m + \boldsymbol{K}_{sc}\boldsymbol{W}\boldsymbol{\Psi}_m & \boldsymbol{K}_{ss} \end{bmatrix},$$

$$\boldsymbol{\xi} = \begin{bmatrix} \boldsymbol{a}_m \\ \boldsymbol{q}_s \end{bmatrix}$$ – hybrid co-ordinates of the whole system,

$$\boldsymbol{f}_{\xi} = \begin{bmatrix} \boldsymbol{\Psi}_m^T(\boldsymbol{f}_m + \boldsymbol{W}^T\boldsymbol{f}_c) \\ \boldsymbol{f}_s \end{bmatrix}$$ – 'hybrid' forces of the system.

Relationships (5)-(10) showed, that for a performance of dynamic analysis in hybrid co-ordinates, here is required matrix $\boldsymbol{\Omega}_m$ of angular natural frequencies and matrix $\boldsymbol{\Psi}_m$ of corresponding normal modes of the modal subsystem. The latter are time-invariant, because that modal subsystem still remains stationary. In order to determine the matrices above, we can apply:

- computer software for calculation of eigenfrequencies and corresponding normal modes of such systems which are idealized discretely. In practise, we utilize high-degree-of-freedom calculation models, created with a use of the finite element method;
- methods of experimental modal analysis.

Both the approaches are recommended, because of necessity of mutual verification of the results obtained.

Example: For one-side-supported plate, dimensions $135 \times 50 \times 5$mm, made of bronze CC3331G, natural frequencies and corresponding normal modes have been calculated, using the MSC NASTRAN package [7]. Normal modes referred to first four natural frequencies of the CC3331G plate are illustrated (Fig. 3).

Because only first normal mode is important, suitable modal experiment has been performed. Subsequently, modal assurance criterion (*MAC*) is assessed (Fig. 4) using the *FeGraph* package. Good agreement between results of calculation and experimental investigation has been confirmed.

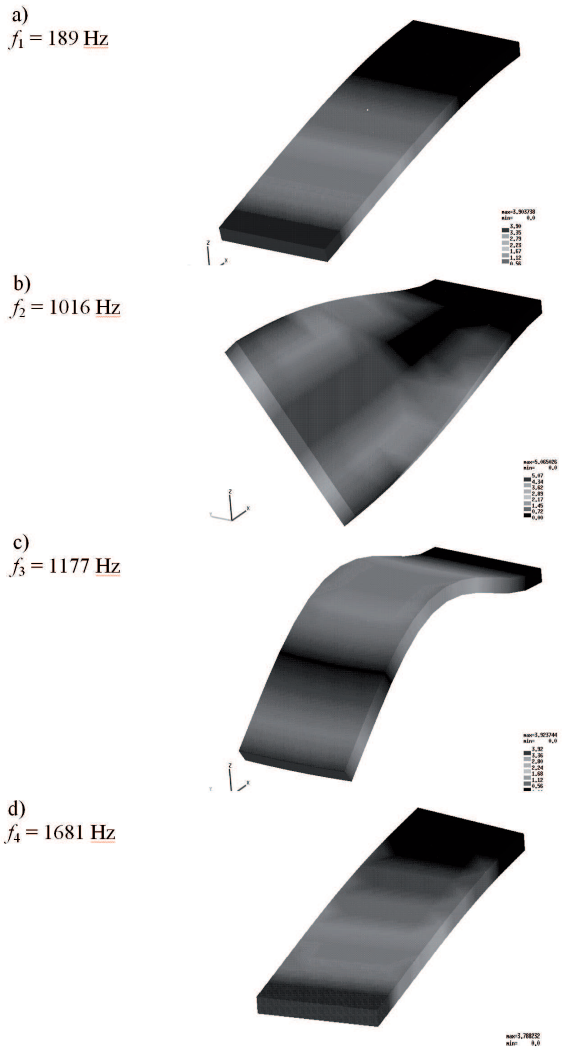

Figure 3. Natural frequencies and normal modes of rectangle plate, b ronze CC331G .

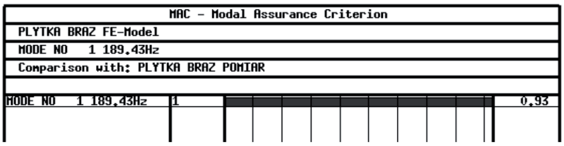

Figure 4. Results of modal assurance criterion (*MAC*) calculation for the bronze CC331G plate.

4. Matching spindle speed of revolution to optimal phase shift

If chatter vibration at exactly one angular frequency $\omega_\alpha = 2\pi f_\alpha$ is observed during cutting process performance, some variables in equation (4) may be expressed as harmonic functions, i.e.:

$$\mathbf{\Delta w}_l(t) = \mathbf{\Delta w}^0_{l,t} \sin(\omega_\alpha t), \tag{11}$$

$$\mathbf{\Delta w}_l(t-\tau_l) = \mathbf{\Delta w}^0_{l,t-\tau_l} \sin(\omega_\alpha (t-\tau_l)). \tag{12}$$

After differentiation of equation (11), with respect to time, we get:

$$d\mathbf{\Delta w}_l(t) = \mathbf{\Delta w}^0_{l,t} \omega_\alpha \cos(\omega_\alpha t) dt. \tag{13}$$

We calculate work of cutting forces of all CEs as:

$$L = \sum_{l=1}^{i_l} \int \mathbf{F}_l^T d\mathbf{\Delta w}_l. \tag{14}$$

Thus, the work done by the component with angular frequency ω_α during time of one vibration period gets a form:

$$L = -\sum_{l=1}^{i_l} (\mathbf{\Delta w}^0_{l,t-T_l})^T \mathbf{D}^T_{Ol} \mathbf{\Delta w}^0_{l,t} \pi \sin(\omega_\alpha \tau_l) = -(\mathbf{q}^0_{t-T_l})^T \underbrace{\sum_{l=1}^{i_l} \mathbf{T}_l^T \mathbf{D}^T_{Ol} \mathbf{T}_l}_{D_0^T} \mathbf{q}^0_t \sin\left(2\pi f_\alpha \frac{60}{z n_\alpha}\right). \tag{15}$$

Sign '–' denotes, that the system losses energy during the work done. It is worthy to note that the work is described in domain of generalized co-ordinates, since that work becomes function of generalized displacements' amplitudes:

$\mathbf{q}^0_t$ – for time-instant t,
$\mathbf{q}^0_{t-T_l}$ – for time-instant $t - \tau_l$.

Minimum energy of vibration will be stored in the system, when absolute value of expression (15) approaches maximum. For a purpose above, following condition is fulfilled:

$$\omega_\alpha \tau_l = \frac{\pi}{2} + 2\pi m, \quad m = 0, 1, \ldots \tag{16}$$

If we rearrange equation (16), we shall derive condition of optimality in the form:

$$\frac{zn_{\alpha}}{60} = \frac{f_{\alpha}}{0.25+m}, \tag{17}$$

where:

f_{α} – observed chatter frequency,
n_{α} – optimal spindle speed, which corresponds to vibration at frequency f_{α},
z – number of cutting edges.

The approach described in this chapter generalizes the Liao-Young condition [6] to a class of multi-degree-of-freedom systems and it converges to the results of the Nyquist vibrostability analysis in a frequency domain. However it provides ability of finding optimal spindle speed taking into consideration an influence of only one resonant peak of chatter vibration. Thus, application of this approach requires separation of chatter resonance with such frequency f_{α}, for which the amplitude is dominant.

As result of all above considerations, following procedure of vibration reduction is suggested.

- Time-domain investigation of a flexible billet, fixed in the holder. As result, transient time response is obtained.
- Detection of chatter frequency by the FFT time-plot analysis. The chatter frequency is expected to be close to a dominant natural frequency of the billet.
- Matching required spindle speed to the chatter frequency being observed (Eq. 17).
- Real performance of the high speed milling process under optimal spindle speed.

5. Experimental investigation

Experimental research was performed on a special stand that allows us to measure displacement of the rotating tool in 2 orthogonal axes and acceleration of up to six points of a machined billet. Spindle rotation speed is also measured.

Experiments were conducted on two machines, that is to say:

- Mikron VCP 600 with maximum spindle speed 20000 rev/min,
- Alcera Gambin 120CR retrofitted with S2M electrospindle with maximum spindle speed 35000 rev/min.

Example 1 Here is performed experimental investigation of vibration surveillance during ball end milling of straight-line grooves on the Mikron VCP 600 milling machine.

The billet was one-side-supported plate, dimensions $135 \times 50 \times 5$mm, made of aluminium alloy EN AW-6101A and sloped with angle 45^0. Cutting parameters are as follows: ball end mill diameter $D = 16$mm, desired depth of cutting $a_p = 0,15$mm, feed per tooth $f_z = 0,01$mm.

Because only first normal mode is important, suitable modal experiment was performed. Then, first natural frequency resulted as $f_n \approx 200$Hz. Following that, a set of optimal spindle speeds has been determined, considering that $f_\alpha = f_n$ and using relationship (17). Result of calculation is $n_\alpha = 4800$rev/min, which lies in a range of allowable spindle speeds. Maximum vibration amplitudes q_{max} and corresponding frequencies for various values of spindle speeds, considered in the experiment, are placed in table 1.

Table 1. Maximum vibration amplitudes q_{max} and corresponding frequencies f_{max}.

Groove no.	n_α[rev/min]	q_{max}[mm]	f_{max}[Hz]
1	3000	0,050	196
2	3900	0,011	191
3	4800	0,009	156
4	5100	0,012	166
5	5400	0,035	176
6	5700	0,025	186
7	6000	0,082	196

Example 2 Similar experiment is performed during ball end milling of straight grooves on the Alcera Gambin 120CR milling machine. The billet was one-side-supported plate, dimensions $150 \times 50 \times 5$mm, made of steel S235JR and sloped with angles 15^0 and 30^0, with respect to the tool. Cutting parameters are as follows: ball end mill diameter $D = 16$mm, desired depth of cutting $a_p = 0,1$mm, feed per tooth $f_z = 0,01$mm.

Because only first normal mode is important, suitable modal experiment was performed. Then, first natural frequency resulted as $f_n \approx 186$Hz. Following that, sequence of optimal spindle speeds has been determined, considering that $f_\alpha = f_n$ and using relationship (17). Result of calculation is $n_\alpha = 22324$rev/min. Although the latter is much higher than in the previous experiment, however it lies in a range of allowable spindle speeds. Maximum vibration amplitudes q_{max} and corresponding frequencies for various values of spindle speeds, considered in the experiment, are placed in table 2.

Table 2. Maximum vibration amplitudes q_{max} and corresponding frequencies f_{max}.

Groove no.	n_{α}[rev/min]	Tilt angle	q_{max}[mm]	f_{max}[Hz]
1	22324	15^0	0,00033	199
2	24324	15^0	0,01265	189
3	20324	15^0	0,03220	189
6	22324	30^0	0,00037	189
7	24324	30^0	0,01186	188
8	20324	30^0	0,02199	188

6. Conclusions

The method of vibration surveillance during machining flexible details by matching the spindle speed to optimal phase shift is developed with success. Thanks to that, vibration surveillance appears efficient at all. Modal model of the workpiece whose parameters are determined either solving an eigenvalue problem of structural model, or using the methods of experimental modal analysis, allows us to determine optimal value of the spindle speed. Results of experimental investigation on the Mikron VCP 600 milling machine, as well as on the Alcera Gambin 120CR machine, mean to be in support. Hence amplitude values for chosen optimal spindle speeds become relatively smaller than for the other ones. Quality of machining is improved in significance as well.

References

[1] J. Tomkow: Vibrostability of machine tools. Warsaw, The Scientific and Technical Publication, 1997.

[2] K.J. Kaliński: Vibration surveillance of mechanical systems which are idealised discretely. Gdansk, The Publication of Gdansk University of Technology, 2001.

[3] K.J. Kaliński, T. Kucharski and S. Sawiak: A new method for suppression of chatter vibration by programmed spindle speed control. *3rd Int. Conf. on Metal Cutting and High Speed Machining*, Metz, France, **I** (2001), 241-250.

[4] K.J. Kaliński: The spindle speed optimal control as a mean of chatter vibration surveillance. *Int. J. Mech. Prod. Systems Eng*, Metz, ENIM, (2003), 30-40.

[5] K.J. Kaliński and M. Galewski: Vibration surveillance during machining processes with a use of the spindle speed linear-optimal control. Theory of Machines

and Mechanisms (Ed. J. Wojnarowski and T. Uhl), Krakow, Chair of Robotics and Machine Dynamics AGH, **2** (2004), 71-76.

[6] Y.S. LIAO and Y.C. YOUNG: A new on-line spindle speed regulation strategy for chatter control. *Int. J. Mach. Tools Manufact*, **36**(5), (1996), 651-660.

[7] K.J. KALINSKI and M. CHODNICKI: Vibration surveillance by the hybrid system's optimal control on example of a cutting process. Theory of Machines and Mechanisms (Ed. J. Wojnarowski and T. Uhl), Krakow, Chair of Robotics and Machine Dynamics AGH, **2** (2004), 197-202.